U. S. Geological Survey.

REPORTS-OPEN FILE SERIES, no. 1019: 1968.

U. S. Geological Survey.

Reports-open file series, no. 1019 : 1968

anal. ok
sl

Accompanies

Weld - Int. 2905
(200)
R290
no. 1019

U. S. GEOLOGICAL SURVEY
Washington, D. C.
20242

For release APRIL 15, 1968

The U. S. Geological Survey is releasing in open files the following reports. Copies are available for consultation in the Geological Survey Libraries, 1033 GSA Bldg., Washington, D.C. 20242; Bldg. 25, Federal Center, Denver, Colo. 80225; and 345 Middlefield Rd., Menlo Park, Calif. 94025. They are also available for consultation in other offices as listed:

1. Availability of palynological material from Naval Petroleum Reserve No. 4, VI: South Barrow Test Well No. 3, by Richard A. Scott. 1 p.

2. Preliminary outcrop map, Rochford and vicinity, Black Hills, South Dakota, showing locations and values of samples analyzed selectively for Au, As, and Cu, by R. V. McGehee, R. W. Bayley, and R. White. 1 sheet, scale 1:24,000. State Geological Survey, Science Center, University of South Dakota, Vermillion, S. Dak. 57069; 1012 Federal Bldg., Denver, Colo. 80202. Material from which copy can be made at private expense is available at this Denver address.

3. Preliminary lunar exploration plan of the Marius Hills region of the Moon, by T. N. V. Karlstrom, J. F. McCauley, and G. A. Swann. 42 p., 3 pl., 3 figs., 2 tables. 601 E. Cedar Ave., Flagstaff, Ariz. 86001.

4. Aerial infrared images of the Geysers geothermal steam field and vicinity, Sonoma County, California, by R. M. Moxham. 3 p., 1 fig., 7 photographs. 601 E. Cedar Ave., Flagstaff, Ariz. 86001.

5. Infrared imagery and radiometry--Summary report, December 1967, by R. M. Moxham, G. W. Greene, J. D. Friedman, and S. J. Gawarecki. 29 p., 35 figs., 1 table. 601 E. Cedar Ave., Flagstaff, Ariz. 86001.

6. Astrogeologic Studies, Annual Progress Report, July 1, 1965, to July 1, 1966. Parts A, B, C, D, and 3 map supplements (12 maps). 601 E. Cedar Ave., Flagstaff, Ariz, 86001; 602 Thomas Bldg., Dallas, Texas 75202; 8102 Federal Office Bldg., Salt Lake City, Utah, 84111; 1012 Federal Bldg., Denver, Colo. 80202; 7638 Federal Bldg., Los Angeles, Calif. 90012; 504 Custom House, San Francisco, Calif. 94111; 678 U.S. Court House Bldg., Spokane, Wash. 99201; 108 Skyline Bldg., Anchorage, Alaska 99501.

UNITED STATES
DEPARTMENT OF THE INTERIOR
GEOLOGICAL SURVEY

INTERAGENCY REPORT NASA-105

INFRARED IMAGERY AND RADIOMETRY

SUMMARY REPORT

DECEMBER 1967

by

Robert Moxham 1919-
R. M. Moxham
G. W. Greene
J. D. Friedman
S. J. Gawarecki

Arlington, Virginia

This report has not been edited or reviewed
for conformity to Geological Survey standards.

Work performed under NASA
CONTRACT NO. T-65754-G

U. S. GEOLOGICAL SURVEY

Released to open files

CONTENTS

TABLE

ILLUSTRATIONS

16. Photo of pyrheliometer (left) amplifier-calibrator (center) and EA recorder (right).

17. Photo of pyrheliometer calibrator-amplifier.

18. Graph showing time vs first light (CdS) sunrise (pyrhel.) and surface temperature rise.

19. Graph showing performance of liquid nitrogen black body.

20. Emissivity measuring system. Emissivity box (A) with upper mirror (B), lower mirror (C) and heater (D). Radiometer head (E) is connected to radiometer (F) at right. The heater controller (G) is at the left. Three rock samples (H) prepared for laboratory testing are shown in foreground.

21. Thermal conductivity measuring system. Controlled temperature water baths (A) and (B) maintain a constant temperature gradient in stacks (C) and (D), shown with insulated jackets in place. Pressure is applied by hydraulic jack (E) and measured by means of gage (F). Thermistor circuits are selected by switch (G) and resistances measured by the Wheatstone bridge (H) and null detector (I).

22. Graph showing anomaly and background surface temperatures measured with multiple probe sequencer at The Geysers.

23. Four levels of density "sliced" with a Tech/Ops quantizer, from IR image of The Geysers. Hottest targets at top, cooler surfaces added by the succeeding three increments.

24. Geographic features superimposed upon level slice (fig. 23). Present northwestern steam production limit is about at center of image. Thermal anomalies extend beyond this limit.

25. IR images at Taal Volcano, Philippines (white=hot).

26. IR image of Potomac River showing warm sewage plant effluent (A) and power plant effluent (B). (white=hot).

27. Infrared image of Balayan Bay, Luzon Island, Philippines.

28. IDT black and white density map of fig. 27.

29. IDT color density map of fig. 27.

30. Rear view of MDT showing color attachment: A=light compartments. B=photocell housing. C=chassis. D= "Dial-lite" spring clip attachment to recording pen arm.

31. Side view of MDT showing color attachment: A=photocell relay. B=lamp socket. C=light compartment switch. D=main light switch. E=photocell circuit bypass switch. F=mounting bracket.

32. Details of light compartment.

33. Details of photocell housing and attachment.

34. Wiring diagram of color attachment.

35. Tech/Ops density map of figure 27.

Introduction

Full utilization of infrared data from space in earth resources applications requires knowledge of abnormal geothermal environments and of the thermal behavior of earth materials. Through classical geophysics much has been learned of earth interior heat flow. But most of this knowledge pertains to "normal" geological environments. In fact, areas having abnormal geothermal gradients usually are deliberately avoided in classical geophysics as they involve intractable problems. The total heat flow in such areas moreover, is not very consequential for the whole earth. Consequently some of the most interesting space applications must deal with the surface manifestations of highly abnormal geothermal gradients, about which we know rather little.

One of the primary efforts of the Infrared Laboratory, therefore, has been to develop instrumentation to measure a) appropriate thermal properties in the field and in the laboratory and b) meteorological parameters that effect IR transmission. The first part of this report deals with the instrumentation, followed by a brief summary of topical studies undertaken and some methods being developed for image processing.

Instrumentation

A. Surface temperature measurements

1. Thermometry--The geologic targets for IR scanning from aerial and space platforms are sufficiently large that some rather unconventional techniques are required for temperature measurements.

Thermistors are widely used for surface temperature measurements though no one has devised a completely satisfactory technique. In fact, if the surface is defined as the air-earth interface, its temperature by thermometric methods is hardly attainable. One usually must settle for a measurement at some small depth up to a centimeter perhaps in unconsolidated materials. On solid rock the thermistor must be somehow attached or embedded in the surface. In either case, thermistors from 2 to 8 mm. diameter are usually used. (figure 1) We employ almost exclusively the Yellow Springs Instrument Co., 400 series, as they have desired stability and precision and moreover are interchangeable in several measurement systems. Controlled temperature baths are used for calibration of these devices.

Large size of the geologic targets in aerial and space IR scanning necessitates thermistor arrays to adequately assess the target's surface temperature. Usually 5 to 10 probes are used.

The electronic thermometer is the ideal instrument for the measurement of temperatures at an untended array station. A wide variety of interchangeable thermistor probes can be used with this device and the electrical output can be recorded using ordinary strip chart recorders. To avoid an unwieldy outflow of paper, we use one recorder or printer for each array.

a. Analog systems--Several types of temperature monitoring systems have been devised, using milliampere or millivolt recorders. The Esterline Angus Model AW recorder is often used because it

has a spring drive and requires no electrical power. (Modifications of the EA meter are discussed below) This recorder will run for several days on one winding and one chart. However, the output of the electronic thermometer is insufficient to operate the EA recorder, so an intermediate amplifier is required.

1. Single probe system--For monitoring a single probe, a system was assembled using a Yellow Springs Instrument Co., Model 43, thermistor, a d.c. differential amplifier (Cemco Model 1755) and a recorder (Esterline Angus Model AW). The amplifier requires 45 to 50 volts to operate, and this is supplied by batteries.

2. Multiple probe systems--A second, more versatile system was assembled using an electronic thermometer with a sequencing switch (Yellow Springs Instrument Co., Model 47) to automatically scan up to eleven thermistor probes in the input. Because this instrument requires 120 volts a.c. for its operation it was necessary to provide this power by adding an inverter (Terado Master) and a 12 volt storage battery to the system. Since a.c. power was available it was decided to use an amplifier operating on this power rather than batteries, so a Cemco Model 1750 amplifier was selected for the second system.

A choice of three scanning programs, covering three, seven or eleven inputs, can be selected and the scanning time can be set to 20 seconds, one minute or five minutes per channel.

According to the manufacturer the accuracy of the system is

1% of the scale span (0-50°C) or 0.5°C. Several procedures have been adopted to insure results as good or better than that. First, calibrations of all probes are checked at regular intervals using an ice bath. Probes that differ from the standard calibration are discarded. Secondly, standard resistors having an almost zero temperature coefficient are used to provide calibration points on the charts during measurements. The resistors are plugged into the input circuits and are measured on each cycle of the sequencing switch. These procedures, together with careful calibration of the equipment, give an accuracy close to ±0.2°C.

The monitoring systems described above use an Esterline-Angus (EA) recorder. The EA recording millimeter is rugged and dependable for field operations. We found however that it is seriously temperature sensitive. Its meter resistance changes about 280 ohms between 0° and 50°C. To compensate for this change a thermistor network was placed in series with the meter circuit as shown in figures 2 and 3. The thermistors were selected so that their change of resistance balances that of the meter. The results are summarized below:

Temp.	Compensator resistance	Meter resistance	Series resistance, Total
- 29°C	577 ohms	1,098 ohms	1,675 ohms
- 20	547	1,148	1,695
- 10	495	1,204	1,699
0	438	1,260	1,698
10	376	1,316	1,692

20	312	1,372	1,684
30	254	1,428	1,682
40	203	1,484	1,687
50	160	1,540	1,700

Due to the large power requirements of the foregoing system a small compact low power thermistor monitoring unit was designed and several have been built in the IR lab. (figures 4, 5 and 6) Field results have been excellent.

Each thermistor in the array is sampled in sequence by an automatic rotary switch. The rotary switch places the thermistor In a conventional bridge and the bridge imbalance is recorded on an ICA recorder. The sampling period for each thermistor is about 2.5 minutes, fixed by a microswitch attached to the recorder drive gear. The rotary switch is spring driven to minimize power consumption. The ICA recorder is powered by Ni-Cad batteries that will operate the entire unit for several days, and can easily be recharged where 115 AC is available. The entire system will operate unattended for several days.

The system permits measurements over a range of 0°-50°C. Full scale deflection may be adjusted for 0°-50°C or for any 10° interval within the 0°-50° range. This flexibility is very useful; it is common for many summer soil temperatures to have diurnal amplitudes of 30° or 40°C, so that a 0°-50°C full scale deflection is required; water temperatures on the other hand may vary only a few degrees, so that a 10° full scale deflection will give optimum results. On the 0°-50°C range (worst case) the system

gives an accuracy of about 0.5°C, which is quite adequate for most purposes.

b. Digital system--A digital thermistor recording system (figures 7, 8 and 9) was devised to eliminate the time consuming data reduction associated with the analog system. Its advantages are achieved at some sacrifice of mobility and power consumption, however. The electronic components are available from United Systems Inc. We utilize a Zeus one KVA propane-powered 115 volt generator. The system will accomodate up to ten thermistors. We usually adjust the programmer so each thermistor in the array will be sampled at 10 minute intervals. For each sampling, the time is printed as well as each temperature and probe identification number. Temperature ranges of 0°-100°C or 0°-100°F are available. The digital system will operate unattended for 36 hours, being limited by the propane supply.

2. Radiometry--Radiometric temperatures, both surface and airborne are required to solve many problems. Most of these studies involve measurements over an extended period of time. Consequently it is almost mandatory to use an AC radiometer, rather than a DC instrument, to achieve the required stability. We have relied mainly on various modifications of the Barnes IT-2 and IT-3 radiometers. In order to obtain a permanent record of the observations, the radiometer output is fed into an Esterline-Angus recorder in both ground and aerial installations. Use of the external recorder requires that the system be calibrated. The conventional Leslie cube is often difficult to use, especially as ice is required to

achieve the lower temperatures. The device described below has been found exceedingly useful.

a. Electrically controlled black body--Radiometer calibration is often a vexing problem. Commercially available black bodies are either optically unsuitable for the purpose or have too high temperature range. Temperatures down to -15°C are commonly encountered in the field so that a black body should have a comparable low temperature capability. This was achieved through use of a Frigipak as shown in figures 10,11 and 12. The Frigipak is a thermoelectric device whose temperature may be regulated by the polarity and amount of current passed through it. A cone shaped aperture recessed into the Frigipak serves as a black cavity. A thermistor, attached to the hot-cold plate, is fed into a Digitec thermometer to monitor the black body temperature. The black body has a temperature range of -15°C to 100°C which can be held steady to within 0.1°C.

b. Barnes radiometer--The Barnes radiometer has been modified to permit radiance measurements a) at a fixed ground station, b) from a moving truck (see fig. 9) and c) from an aircraft. For a fixed station, the radiometer is operated in a conventional way. For cross-country traverses, the radiometer head is fastened to the cab of a 4-wheel drive truck so that its 3° field of view looks at a ground track along the truck's path. The detector signal is fed to the amplifier and recorder inside the truck. The chart drive of the EA recorder has been replaced by a set of external gears driven by a cable from the truck's speedometer. The chart speed consequently is proportional to the distance traveled, so that the radiometer

record has a constant horizontal scale. The constant scale greatly assists fixing the geographic location of specific points on the record.

The Barnes instruments cover the temperature range -10° to 50°C, which is probably the most useful span for most geologic problems. The EA recorder output therefore has a full scale deflection covering the same range. Some targets such as bodies of water have a much smaller temperature range, however. It is also desirable to be able to resolve much smaller temperature differences over water than over a land surface. To increase the precision of the radiometric system an operational amplifier was incorporated to increase the output signal to the recorder so that full scale deflection is obtained for a 5°C change in radiant temperature. Provision is made in the circuit so that any 5° span can be observed within the overall -10° to 50° range of the radiometer.

c. Airborne IR scanner--The IR scanner system utilized most extensively during this period was the HRB Reconofax IV. The instrument was carried in a Twin Beech operated by the USGS Water Resources Division. In most instances, aerial photos were also obtained in the areas surveyed.

The IR instrumentation was essentially straightforward and will not be discussed. However, one of the principal problems in field operations is to provide a portable compact system for drawing a vacuum on the order of 1 or 2 X 10^{-5} Torr. Though the detector will operate at less vacuum, the desired value will give a greater

hold time. A vacuum system meeting this requirement was devised as shown in figures 13 and 14.

3. Meteorological observations--Relative humidity, air temperatures and insolation are generally made with conventional recording devices, or supplemented by thermistors. Some IR surveys made during early dawn require that the time of first light be known as well as the subsequent time when a perceptible temperature rise occurs at the earth's surface. The surface temperature rise time is recorded by the thermistor surface array and onset of insolation is shown by the pyrheliometer output recorded on an EA meter (figures 15, 16 and 17). First light of dawn is sensed by a cadmium sulfide cell. The cell is placed in series with a 100K potentiometer, a 67 1/2 volt dry cell and an EA meter.

The relation between all of these parameters can then be determined as shown in figure 18.

4. Emissivity measurements

a. Laboratory--Both the spectral emissivity and the integral emissivity in the 2-6μ and 8-14μ regions are of interest for certain IR problems. Spectral emissivities are determined in our laboratory using the Block inteferometer spectrometer. Rock preparation and the spectral measurements are straightforward. The results of this work has been given in detail by Daniels (1967 a and b).

Experiments on the use of a blackbody maintained at liquid nitrogen temperature in the study of spectral emittance of rocks, in situ or in the laboratory, have been made. Providing the sample

studied and a reference blackbody assume the same arbitrary temperature, the method provides a rather simple, absolute determination of spectral emissivity utilizing the Block interferometer type spectrometer. Theory and the detailed results have been given by Daniels and Stoddard (1966).

The liquid nitrogen temperature blackbody was constructed by spraying 3M Velvet Coating black paint over the interior of a 2 3/4" I.D. by 9 1/4" overall height, one pint pyrex dewar. This paint is quite resistant to the thermal shock, whereas Parson's Black flakes at low temperature. Other paints may be found which are superior. The dewar was filled with liquid nitrogen to within a half inch of the top and viewed directly by the interferometer at a distance of approximately two inches. In this configuration a thin, broken water cloud wavers over the liquid surface. This cloud could be eliminated by proper design, but it was observed not to reflect infrared from a hot soldering iron into the interferometer.

The recorder amplitude when the instrument views this blackbody should depend only upon the detector temperature, and should increase as the detector temperature is increased. Runs with the detector at 29, 34, 40, 45 and 50°C showed this effect. Figure 19 shows the ratio of the recorder amplitudes with the detector at elevated temperatures to the amplitude at 29°C for selected wavelengths. The increase is greater than the corresponding ratios of the intensity of detector emission at these temperatures as calculated from the Planck formula. It had been anticipated that amplitude ratios

smaller than corresponding emission ratios would measure the reflection of room radiation by the cold blackbody. The reverse behavior is apparently due to an increase in responsivity of the detector with temperature. The necessary increase in responsivity is also shown in figure 19and is, as yet, unexplained.

b. Field--Field measurements of emissivity can be made by means of an emissivity box modeled after the instrument described by Buettner et al., (1965). The device is a cylinder with its inside surfaces highly polished and gold plated (fig. 20). At the top of the cylinder is a controlled temperature heater which maintains the grooved and black-painted lid at a constant temperature, higher than that of the surface being measured. A Barnes IT-3 radiometer is installed on the lid so that it can "look" through a hole in the lid. Polished, gold plated mirrors can be slipped into positions parallel to and just below the heater surface, and parallel to the heater surface and just above the surface being measured. The upper mirror has a hole in the center so that the radiometer can "look" through it.

The instrument and the method of making measurements has been slightly modified from that described by Buettner et al., (1965). The box is placed on the surface to be measured and the radiant temperature of the surface is measured by the radiometer, first with the top mirror covering the heater and then with the mirror removed. A third measurement is made of the radiant temperature of the heater by slipping the bottom mirror into position below the

heater. Finally, the radiant temperature of the top mirror is measured by slipping it part way in so that it covers the radiometer. A spot of Parson's black on the top surface of the mirror is used as a target for this measurement.

The emissivity of the surface being tested is calculated by the equation:

$$\varepsilon_s = 1 - (T_{sb} - T_{sm}) / (\varepsilon_b T_b - \varepsilon_m T_m + r_b T_{sb} - r_m T_{sm})$$

where

ε_s = emissivity of surface under test
T_{sb} = equivalent black body temperature of surface under test when heater is over the surface
T_{sm} = equivalent black body temperature of surface under test when mirror covers heater
ε_b = emissivity of black heater surface = 0.985 (assumed)
T_b = equivalent black body temperature of heater
ε_m = emissivity of gold mirror surface = 0.01 (assumed)
T_m = equivalent black body temperature of top mirror
r_b = reflectivity of heater surface = $(1 - \varepsilon_b)$ or 0.015
r_m = reflectivity of gold mirror surface = $(1 - \varepsilon_m$ or 0.99

Emissivities in the 8-14 micron band of a number of rock surfaces have been measured by this method with reasonably good agreement with the results obtained with the infrared spectrometer. (Friedman, 1968)

Thermal conductivity measurements

a. Laboratory--Thermal conductivity measurements are made by the divided-bar, or steady state, method. The apparatus in use was designed and built by personnel of the U. S. Geological Survey Geothermal Studies Project in Menlo Park, California, (fig. 21). It uses two controlled temperature water baths to establish a

uniform heat flow through each of the two stacks of rock specimens and standards under test. This method is much superior to the method used in the classical apparatus (Benfield, 1939; Birch 1950; Beck, 1957), wherein an electrical heater and a cold water bath serve as heat source and sink.

Samples are prepared for testing by cutting slices approximately 0.6 to 1.2 cm thick from rock specimens. A diamond drill is then used to cut discs 3.84 cm in diameter from the slices of rock. The discs are ground and polished until their ends are plane and parallel within ±0.001 cm.

Four rock samples may be handled at one time in the thermal conductivity test, two samples in each stack. Each stack is prepared by placing two rock specimens between three standards of known conductivity. Copper discs into which thermistors can be inserted are placed between the specimens and standards and at each end of the stack. A thin coat of a special compound having high thermal conductivity is used at each interface to reduce thermal resistance.

The stack of discs is then placed between two cylindrical heads. The temperature of each head is maintained at a constant temperature water baths. The lower head is mounted on a hydraulic jack by means of a special hemispherical thrust bearing. Pressure (usually 30 kg cm^{-2}) is applied to the stack by the hydraulic jack to further reduce thermal resistance. After thermistors have been inserted into the copper discs, insulated shields are placed around the stack to reduce lateral heat losses and to isolate the stack from changes in room temperature.

An equilibrium temperature gradient in the stack is usually attained within 15 to 20 minutes. Temperatures are monitored using a wheatstone bridge to measure thermistor resistance and final readings are not made until a steady-state has been attained.

From the measured temperatures the gradient across each standard is calculated. The thermal conductivity at the measured temperatures is known for each standard, hence the heat flow in each may be calculated by the equation

$$Q=\frac{dT}{dz}K$$

In practice there is a small difference in heat flow in each standard because of lateral heat losses (or gains), but if these differences do not exceed a few percent they are neglected. With a known heat flow through the rock specimens and a known gradient across them, the thermal conductivities may then be calculated.

Discs cut from single quartz crystals so that the heat flow is perpendicular to the c-axis (K=0.0153 at 20°C) are used as primary standards. Secondary standards used in the day-to-day measurements are checked against the quartz discs. The most commonly used standard is fused silica (K=0.00325 at 20°C), but also available are standards of isolantite (K=0.0065 at 20°C), mullite (K=0.0098 at 20°C) and alumina (K=0.065 at 20°C). Different standards and different thicknesses of standards are used with different rock samples so that a nearly uniform gradient is maintained across the stack. This tends to reduce lateral heat losses.

An accuracy of ± 5% is usually claimed for this method of

measuring thermal conductivity. Experience has shown that with careful work accuracies of ± 2% may be achieved.

b. Field--Another device for the measurement of thermal conductivity, and used widely for in situ measurements of unconsolidated materials, is the conductivity probe. The probe is a long, thin (length greater than 50 times the diameter) tube, inside of which is a heater wire and a thermistor. The heater extends the full length of the probe and the thermistor is centered longitudinally next to the heater. A heater power supply with a means of measuring the power supplied to the heater, and a means of measuring and recording the temperature changes indicated by the thermistor are required.

Lachenbruch (1957) reviews the development of the thermal conductivity probe and discusses the theory of its operation.

The probe is inserted into the medium to be tested and the temperature as indicated by the thermistor is observed until the temperature or the temperature change with time (drift) is constant. A constant flow of current is passed into the heater and the resulting temperature change shown by the thermistor is recorded.

When the drift-corrected temperatures are plotted against the logarithm of time after heater activation, an approximately straight line is obtained. The thermal conductivity of the test medium is proportional to the inverse slope of this line and may be computed from the test data.

Two sizes of probes are in use at the present time. A small

size (6.4 cm long x 0.1 cm diameter) is designed for use with small, fine-grained soils, and a large size (30 cm long x 0.3 cm diameter) is designed for use with sandy soils.

Standards are being prepared which will enable the probes to be calibrated and checked frequently. Comparisons with results obtained using the divided-bar method will also be possible.

Evaluation of airborne IR scanner measurements

The aerial IR scanner surveys during this reporting period have been made in areas where generally some abnormal geothermal condition exists. The areas fall into several categories 1) geothermal steam fields, 2) volcanoes and hot springs, 3) thermal effluent, 4) structural anomalies. Intensive studies in the Pisgah Crater and Mono Craters area Calif., begun in earlier years, were also brought to completion.

A. Geothermal steam fields--At The Geysers geothermal steam field, Sonoma County, California, the IR data show in detail the surface heat manifestations associated with areas of highly altered, steaming ground (figure 22). More interesting however, is the fact that some thermal lineaments coincide with faults. It was also found that low grade thermal anomalies extend northwestward beyond the known limits of the steam field (Moxham 1967c). These features can only be delineated by level-slicing techniques in data processing, as shown in figures 23 and 24 . Surface temperature measurements with thermistor arrays verify that the IR anomalies here

Table 1.

Summary of field projects, IR Laboratory, FY 1967 - 1968 (thru 1/1/68)

		Field				Laboratory		
Area	State	Air Photo	Continuous Surface T	Spot T	Meteor.	Thermal Conduct	IR Spectra	Automatic Dens. Scan.
Pisgah Crater	Calif.	x	x	x	x	x	x	
Mono Craters	"		x	x	x	x	x	x
San Andreas fault (Carrizo Pl.)	"	x	x	x	x			
The Geysers	"	x	x	x	x	x	x	x
Mt. Lassen	"	x	x	x	x			
Crater Lake	Oregon	x		x				
Cascade volcanoes (Shasta, St. Helens Adams, Rainier)	Calif. Wash.	x						
Salton Sea	Calif.	x	x	x	x			
Lake Erie	Ohio-Mich.			x				
Taal Volcano	Philippines	x		x	x			x
Steamboat Hot Springs	Nevada	x	x	x	x			
Brady Hot Springs a/	"							
Wabuska Hot Springs a/	"							
Manhattan a/	"	x						
Coal Mine fires	Penna	x	x	x	x	x		
Dixie Valley a/	Nevada							

a/ Reconnaissance flight to determine whether additional IR studies should be made.

Note - We obtained IR data for Water Resources Div. in several areas not listed here. We had no part in the planning, data collection or data reduction.

are in fact due to temperature variations, and not to emissivity or some other extraneous factor.

Surveys in other geothermal areas (listed in Table 1) have not yet been fully evaluated.

B. Volcanoes and hot springs--A series of surveys have been made over Taal Volcano, Philippines, following the September 1965 eruption, during the quiescent stage, and following the 1966 eruption (Moxham 1967a). Results indicate that the principal changes in surface temperature stemmed from changes in convective heat transfer by hydrothermal fluids. New hot springs developed along the structurally-controlled northwest and southeast flanks of the 1965 explosion crater (figure 25A). The northwest spring grew in size prior to the 1966 eruption, persisted through that eruption and has since maintained its discharge. The 1965 cinder cone meanwhile showed a persistent rim of hydrothermal activity with some shift in position of maximum discharge. The July 1966 eruptions took place on the rim about midway between two positions of maximum discharge.

C. Thermal effluents--Thermal effluent from sewage disposal plants and from power plants can be very effectively depicted by the IR scanning technique. An example is shown in figure 26. Details of this work are given by Moxham (1967b)

D. Structural anomalies--Infrared imagery (in the 8- to 13-micron band) of the San Andreas fault system in the Carrizo Plain area of California shows that the fault can be clearly traced over most of about 200 miles flown. Variations in soil moisture caused

by the water-barrier characteristics of the fault zone, as well as vegetation differences related to soil moisture and microtopography are factors influencing visibility of the fault in the IR imagery. Also identified on the imagery and useful in analyzing offset on the fault are (1) offset segments of ancient stream channels disrupted by movement on the fault, (2) landslide terrain, and (3) numerous soil and Tertiary bedrock units. Imagery obtained 1-2 hours before sunrise is considered most useful for the fault studies. Details of this study have been given by Wallace and Moxham, 1967.

E. Pisgah Crater, Calif.--The infrared survey of the Pisgah Crater Area, San Bernardino County, California was primarily undertaken to establish parameters by which rock types, structures, and textures peculiar to this locale could be recognized or differentiated. A secondary purpose was to provide an adequate evaluation and calibration of airborne and ground-based instruments used in the survey.

Pisgah Crater and its vicinity was chosen as one of the fundamental test sites for the NASA remote sensing program because of its relatively fresh basaltic flows and pyroclastics. Its typical exposure of basalt also made it a possible lunar analogue.

The area of study is in the southern Mojave Desert, about 40 miles east-southeast of Barstow, California. It includes the Pisgah and Sunshine lava fields and their associated cinder cones, Lavic

dry lake, alluvial fans, and some exposed older volcanic and plutonic rocks.

Infrared surveys were flown February 11 through 13, 1965 and August 4 and 5, 1966. The initial survey was flown by NASA personnel aboard the NASA 926 Convair 240 aircraft. Because of technical problems with the infrared scanners (4.5 - 5.5 and 8 - 14 micron bands) and with certain ground instruments, most of the imagery and ground temperature data obtained during the initial survey were of little value. However, during the August 1966 survey excellent imagery in the 8 - 14 micron (μ) band region of the spectrum was acquired by the Geological Survey. The scanner was mounted in a Beech D-18 aircraft provided by the Survey's Water Resources Division. Likewise, more reliable ground data was obtained at this time owing to improved instrumentation and technique.

The infrared survey of the Pisgah Crater area has shown that the 8 - 14 micron data can complement aerial photography, radar, and other sensors to provide useful geologic information.

The most useful infrared data was obtained from imagery flown during 3 of the 6 flight periods: 2000 (post-sunset), 0400 (pre-sunrise), and 1200 (mid-day). The largest amount of information on geologic thermal parameters was obtained from imagery flown at 2000, shortly after sunset, when optimum thermal contrast occurred between various terrain materials. However, no single image provided all the thermal contrasts potentially present in the area

because of the complex diurnal thermal cycle. At 2000, the best temperature contrast occurred between the basalt and surrounding unconsolidated sediments, the pumice cones and wash, and other bedrock units. Where adjoining basalt flows within the lava field differ due to surface texture, they may be readily distinguished in the post-sunset and mid-day imagery, and to a lesser degree, on the imagery obtained at other times.

The Lavic playa exhibits much more detail on all images than existing conventional black and white photography and other sensor imagery, primarily due to moisture differences caused by slight lithologic variations. Zoning and detail within the playa shows best on post-sunset and mid-day images. Recently moistened active drainage courses on the adjoining alluvial fan to the east of the playa are easily discerned on the daytime images. Moist areas in some alluvium also suggest the presence of ephemeral springs.

The Pisgah fault was shown on midnight and pre-dawn imagery to have to have a complex fracture pattern where it cuts the Sunshine lava flows. This fracture pattern is better seen on IR imagery than on aerial photographs because fissure-like openings and small scarps with their associated rubble slopes act as black body cavities and remain relatively warm due to delayed radiation cooling to the cold night sky. Collapsed lava tubes and fissured areas on the Pisgah lava field react in the same manner as the fault in the Sunshine lavas.

Most of the thermistor probe and radiometer data recorded on

the basaltic rocks and lake bed verify the relative radiant temperatures as shown on the infrared imagery. The ground temperature measurement program conducted during the period of the aerial infrared survey has shown that basic techniques and instruments need only minor refinements.

The details concerning this work will be given in Interagency Report NASA - 99 (Gawarecki, 1968) which has been completed and is being drafted. Several reports on various aspects of this study have been given in previous Technical letters.

F. Mono Craters area, Calif.--The Mono Craters area, Calif., was selected for airborne infrared scanning radiometer experiments because of the exposure in this area of a variety of lithologies having different physical and thermal properties as well as a diversity of textural and morphologic features. Infrared surveys were undertaken in 1965 and 1966 to measure variations in infrared emission from the surface in the 4.5 - 5.5μ and 8-14μ bands. Areal variations in emission from the surface were registered on film as differences in image tonal density. In addition, variations of surface radiant-temperature with time during the diurnal cycle were recorded at several selected localities.

Three north-south flight lines were used to control the infrared surveys made with a Reconofax IV scanner mounted in the Geological Survey's twin-engine Beechcraft on July 27-28, 1966. Rotating high-intensity beacons marked for the flight lines during night surveys. Several ground instrument monitoring stations were set

up along or close to the flight lines at geologic contacts between selected lithologic map units. The ground stations were designed to obtain observations on diurnal temperature variations of selected natural lithologic surfaces. Two types of instrument systems were operated simultaneously with survey overflights: Barnes IT-3 and IT-2 fixed-field radiometers recording continuously on an Esterline-Angus strip-chart recorder, and sequencer thermistor-probe systems also recording on Esterline-Angus recorders. Other equipment included recording tempscribe thermographs and a recording Epply pyrheliometer (figure 16) to determine variations in the incident radiant flux at the terrestrial surface, 1/ recording thermographs for determining ambient temperature variations and a velometer for near-surface wind variations. Diurnal surface-temperature curves were established from these ground measurements.

Infrared survey overflights were made at 4-hour intervals during a 24-hour cycle. Selected frames of infrared imagery obtained by this method were scanned in the laboratory at magnifications of five and ten times by a double-beam recording isodensitometer to obtain color printouts of film emulsion density increments -- roughly equivalent to form-line isoradiance maps with a variable contour interval. Density profiles were also obtained. A comparison

1/ The major part of the incident radiant solar flux is recorded by the Epply pyrheliometer. The transmission capability of the glass bulb is above 50 percent for wavelength from 305Å to 4.4μ and is above 90 percent for wavelengths between 360Å and 2.6μ.

between image tonal density differences and diurnal surface-temperature curves for various materials established from ground observations was the next step. Thermal properties and infrared integrated bandpass emissivity determinations on rocks of the Mono area were compiled to aid in construction of theoretical diurnal surface-temperature curves using equations for a physical model. The theoretical warming and cooling curves obtained were compared with those obtained by ground observation to estimate the degree to which surface temperature variations and infrared emission variations are influenced by differences in the thermal inertia (φ) of natural materials. Finally, anomalous thermal patterns recorded on the infrared imagery, but not attributable to insolation variations, thermal-parameter, or emissivity differences of materials, were interpreted geologically. The observed thermal patterns can be grouped as follows:

1) Thermal anomalies due to convective heat loss detected when the temperature difference between the heat source and surrounding terrain was maximal, e.g., hot springs and a warm effluent at Black Point.
2) Daytime radiant temperature differences resulting from variations in the incident radiant solar flux as a function of microrelief and morphology of the surface.
3) Night time radiant temperature differences resulting from contrasts in physical and thermal properties of various lithologic units and water expressed as different rates of change in emission, e.g., between olivine

basalt lapilli-ash beach deposits, lacustrine carbonate deposits and water along the north shore of Mono Lake at Black Point.

The detectability of the third group of thermal patterns in the Mono Lake area is of the greatest experimental interest. Night time radiative heat loss is dependent upon the $1-r_o/\beta$ ratios as a property of materials, the total radiant energy incident on the surface during daytime (J_o as a function of topography) and integrated emissivity ($\bar{\varepsilon}$) as a function of surface roughness and blackbody cone effects, and to a lesser extent, of composition.

Several hot springs and fumaroles around the periphery of a Quaternary andesitic volcano on Paoha Island in Mono Lake, Calif., are controlled by faults transecting the crater remnant. Relative intensity of thermal emission from the hot springs and fumaroles was mapped by airborne infrared imagery and isodensitracer scanning techniques. On the basis of temperature and rates-of-flow measurements the total thermal-energy release may be greater than 18×10^6 cal per sec.

Detailed results of the investigations are given in a report which is now being prepared for reproduction (Friedman, 1968). Previously transmitted Technical Letters have described various aspects of the work as it progressed (e.g. Daniels, 1966; Friedman, 1966 a and b).

In addition to the field studies described above a laboratory study of far infrared luminescence was undertaken to determine whether such emission might be important under certain conditions of surface illumination by solar, x-ray and ultraviolet energy.

The results were generally negative, though some lower limits were established (Stoddard, 1967).

Data processing

A. Film density analyzers

1. Joyce-Loebl IDT-MDT--Images produced by IR scanners at the present state-of-the art are not quantitative. However it is highly desirable to have some means of objectively assessing image density, which in turn is related to terrain radiance. Recording microdensitometry is a useful technique for this purpose. A Joyce-Loebl Microdensitometer-Isodensitracer (MDT-IDT) has been modified to adapt it to our special needs (Turner and Boynton, 1968).

The MDT-IDT produces a map of the IR film density, wherein density levels are indicated by appropriate symbols, either space, dot, or dash (figures 27 and 28). It is convenient to consider the boundaries of density levels as contour lines. The MDT-IDT offers several advantages in image analysis. It quantizes density levels and variations in level by direct comparison against a standard density wedge. This avoids the usual errors connected with subjective visual comparisons and allows accurate correlation of density over wide areas. Moreover, by proper choice of contour interval, small scale variations in density can be enhanced. These maps are easily reproduced as illustrations or slides, avoiding problems of tonal value distortion in reproduction, or in viewing, the original film. As a derivative of the original imagery, it allows an unclassified presentation of data that might otherwise be classified.

The MDT-IDT in conventional operation generates a black and white map using only three symbols -- space, dot and dash. Where density gradients are steep or rapidly changing, we found the 3-mode black and white map difficult to interpret. An attachment was developed in this laboratory which divides the density range into seven color-coded divisions1/ (fig. 29). The system employs seven lights (one for each division) placed along the path of the microdensitometer pen (figures 30, 31, 32 and 33). A photocell attached to the microdensitometer pen allows the isodensitracer to record only when the photocell is in the light path. Using the number 12 pen encoder (commutator) provided with the instrument, the full scale range gives 21 different density increments (seven major divisions each with a space, dot and dash pen made). In order to give each major density division a color, it is necessary to make a separate run over the entire area for each division.

The color attachment consists of (a) a bank of lights (placed along the path of the MDT pen); (b) a photocell (attached to the MDT pen arm and scanning the lights); (c) a relay (which is controlled by the photocell and which allows the IDT circuit to print the dot or dash corresponding to the commutator position); and (d) a power supply for the light compartments, photocell, and relay (fig. 34).

2. the Tech/Ops image quantizer--Isodensity maps have also

1/ A four-color IDT is now available commercially.

been made with the Tech/Ops Inc. image quantizer. This is a facsimile recording-type machine with specimen film and recording paper attached to a rotating drum. A light beam, either reflected or transmitted, is detected by a photomultiplier. Recording is by an electrical signal impressed on a stylus in contact with sensitized recording paper.

The image quantizer has four density modes which are printed as white, light grey, dark grey and black. The total density range and density increments are adjustable by steps. The minimum scanning aperture of 100, lack of magnification, and the single color printing make it somewhat inflexible for our purpose. However, it has the distinct advantage of rapid recording. An isodensity map of Balayan Bay, Philippines made by the image quantizer is shown in figure 35 (see also figures 23 and 24).

REFERENCES

Reports prepared by the Infrared Laboratory

Daniels, D. L., 1966, Infrared spectral emittance of rocks from the Pisgah Crater and Mono Craters areas, California: U. S. Geol. Survey Tech. Letter NASA-13.

Daniels, D. L., 1967a, Additional infrared spectral emittance measurements of rocks from the Mono Craters Region, California: U. S. Geol. Survey Tech. Letter NASA-90.

Daniels, D. L., 1967b, New infrared spectral emittance measurements of rocks from the Mono Craters, California: U. S. Geol. Survey Tech. Letter NASA-13 (Supplement).

Daniels, D. L., and Stoddard, A. E., 1966, Liquid nitrogen blackbody for spectral emittance study: U. S. Geol. Survey Tech. Letter NASA-57.

Friedman, J. D., 1966a, Geologic map of the Mono Craters area, California: U. S. Geol. Survey Tech. Letter NASA-12.

Friedman, J. D., 1966b, Composition of basalt flows at Pisgah Crater, California: U. S. Geol. Survey Tech. Letter NASA-20.

Friedman, J. D., 1968, Thermal anomalies and geologic features of the Mono Lake area, California, as revealed by infrared imagery: U. S. Geol. Survey Tech Letter NASA-82.

Gawarecki, S. J., 1968, Infrared survey of the Pisgah Crater area, San Bernardino County, California: U. S. Geol. Survey Interagency Report NASA-99.

Moxham, R. M., 1967a, Changes in surface temperature at Taal Volcano, 1965-1966: Bull. Volcanologique, v. 31, p. 215-234.

Moxham, R. M., 1967b, Aerial infrared surveys in water resources studies: Proc. United Nations Symp. on New Methods in Geophysics, (in press). (also U. S. Geol. Survey Tech. Letter NASA-74)

Moxham, R. M., 1967c, Aerial infrared survey at The Geysers geothermal steam field, California. (Abstract): Geophysics (in press).

Stoddard, A. E., 1967, Far infrared luminescence: U. S. Geol. Survey Interagency Report NASA-91.

Turner, R. M., and Boynton, G. R., 1968, Film density analyzers for infrared investigations: U. S. Geol. Survey Interagency Report NASA-94.

Wallace, R. E., and Moxham, R. M., 1967, Use of infrared imagery in study of the San Andreas fault system, California: U. S. Geol. Survey Prof. Paper 575-D, p. 147-156.

Other reports

Beck, A., 1957, A steady-state method for the rapid measurement of the thermal conductivity of rocks: J. Sci. Instr., v. 34, p. 186-189.

Benfield, A. E., 1939, Terrestial heat flow in Great Brittain: Proc. Roy. Soc. London, A, v. 173, p. 428-450.

Birch, Francis, 1950, Flow of heat in the Front Range, Colorado: Bull. Geol. Soc. America, v. 61, p. 567-630.

Buettner, K. K. K., and Kern, C. D., 1965, The determination of infrared emissivities of terrestrial surfaces: J. Geophysical Res., v. 70, p. 1329-1337.

Lachenbruch, A. H., 1957, A probe for measurement of thermal conductivity of frozen soils in place: Trans. American Geophysical Union, v. 38, p. 691-697.

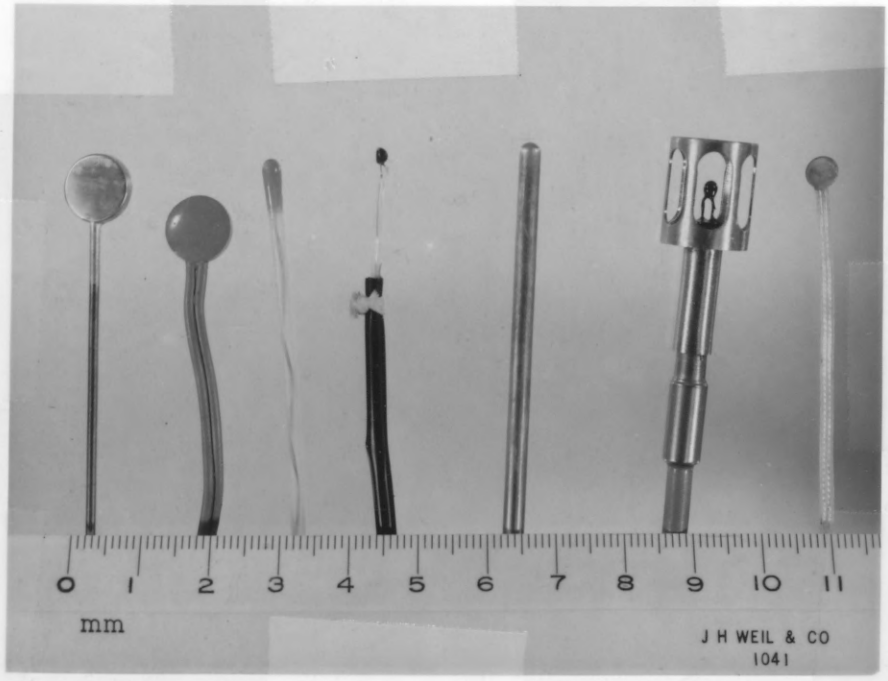

Figure 1. Thermistors used for soil and air temperature measurements.

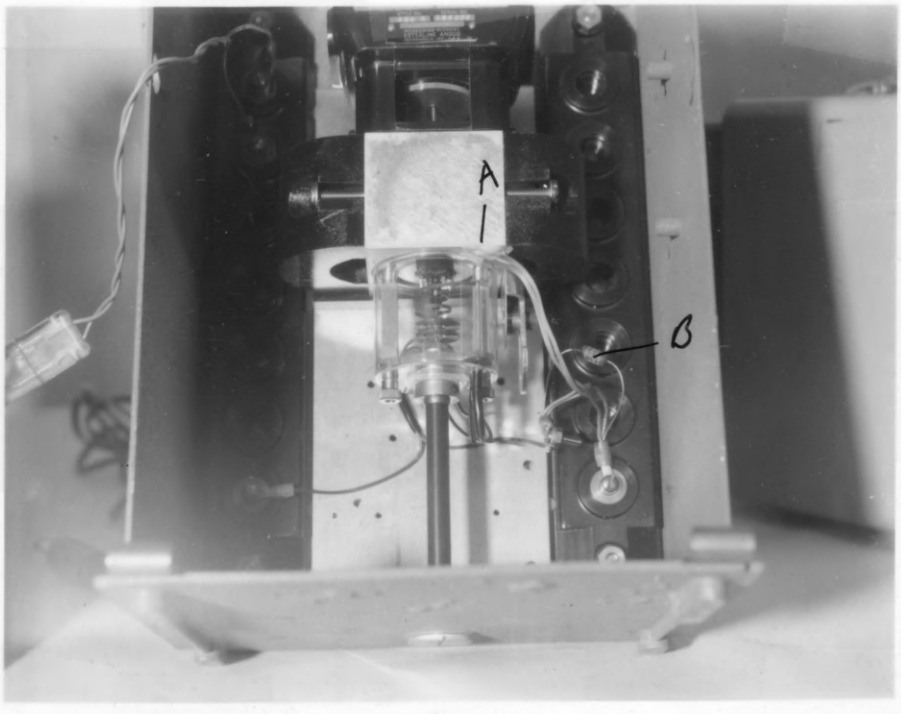

Figure 2. Photo of EA meter showing modifications. A=thermistors; B=series resistor.

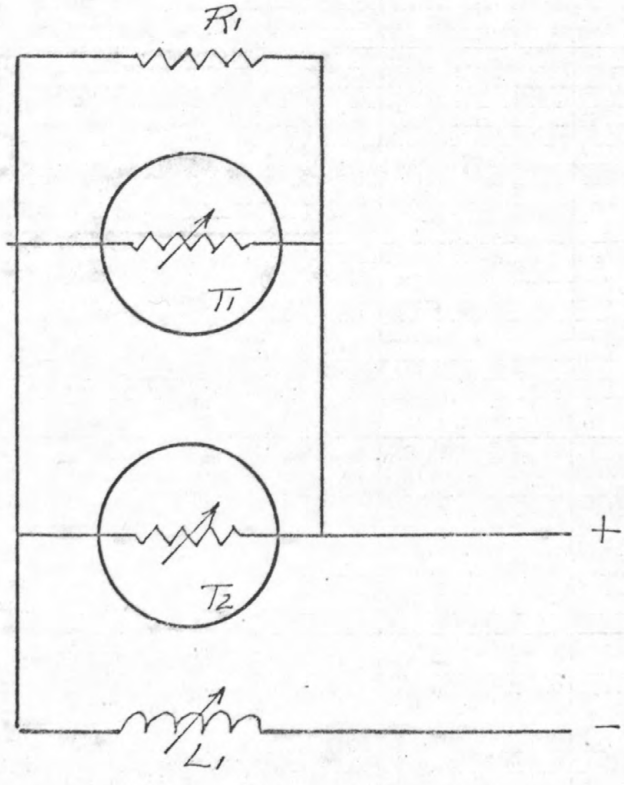

R_1 = 649 Ω
T_1 = YSI 44003
T_2 = YSI 44003
(1000 Ω @ 25°C)
L_1 = EA meter

Figure 3. Temperature compensator for Esterline-Angus recorder

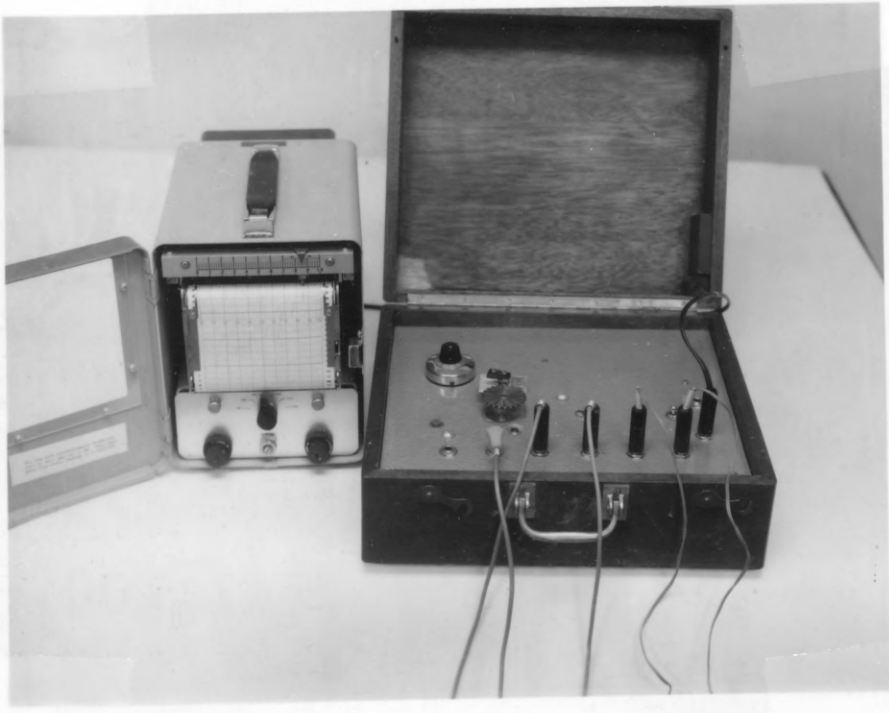

Figure 4. Multiple temperature probes with sequencing bridge (right) and ICA recorder (left).

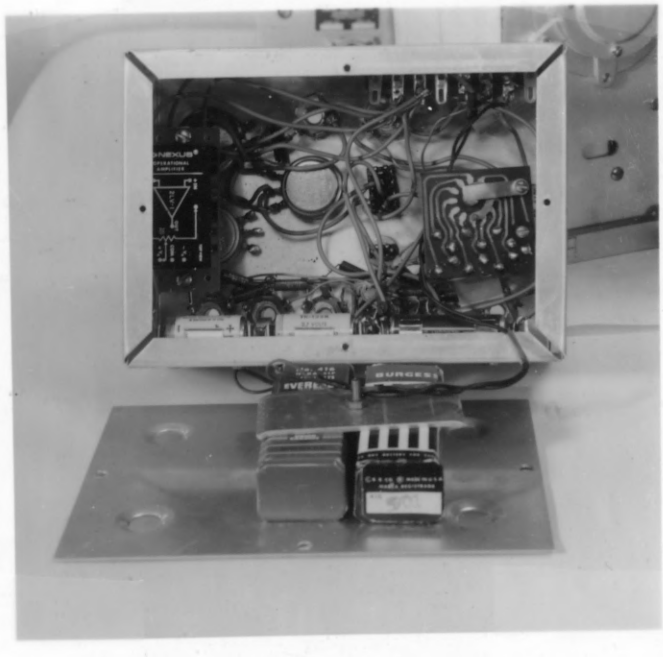

Figure 5. Bottom view of sequencing bridge and amplifier for EA recorder.

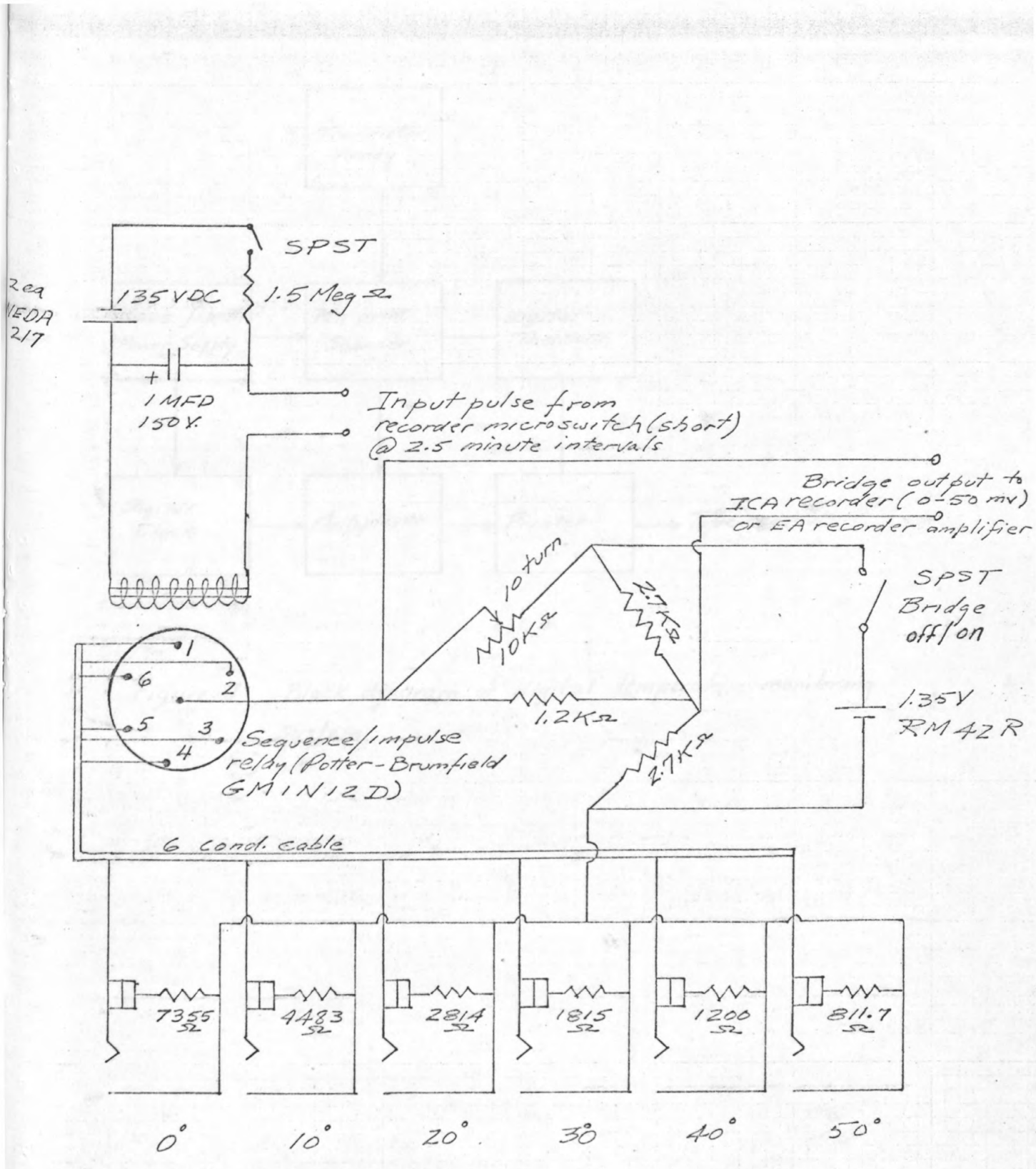

Figure 6. Wiring diagram of sequencing bridge.

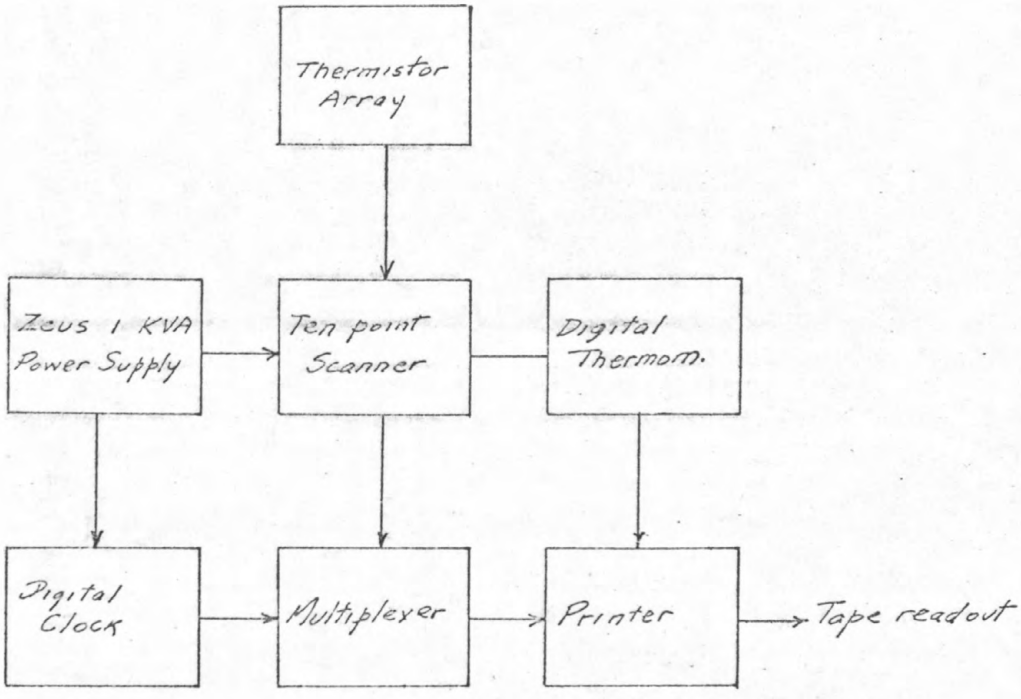

Figure 7. Block diagram of digital temperature monitoring system.

Figure 8. Field installation of digital equipment.

Figure 9. Field station with monitoring equipment. Left to right, multiple probe sequencer with ICA recorder, pyrheliometer with EA recorder, digital sequencer with Zeus power supply and propane tank. Truck in background shows radiometer head mounted above cab.

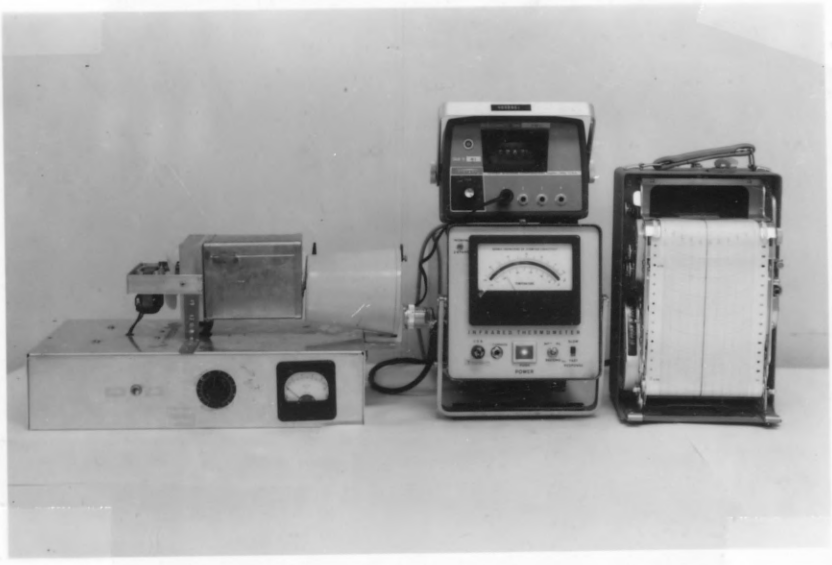

Figure 10. Photo of lab set-up using electrically controlled black body (left); Digitec digital thermometer (center top) Barnes IT3 amplifier (center bottom) and EA recorder (right). Radiometer head is "looking" into black cavity.

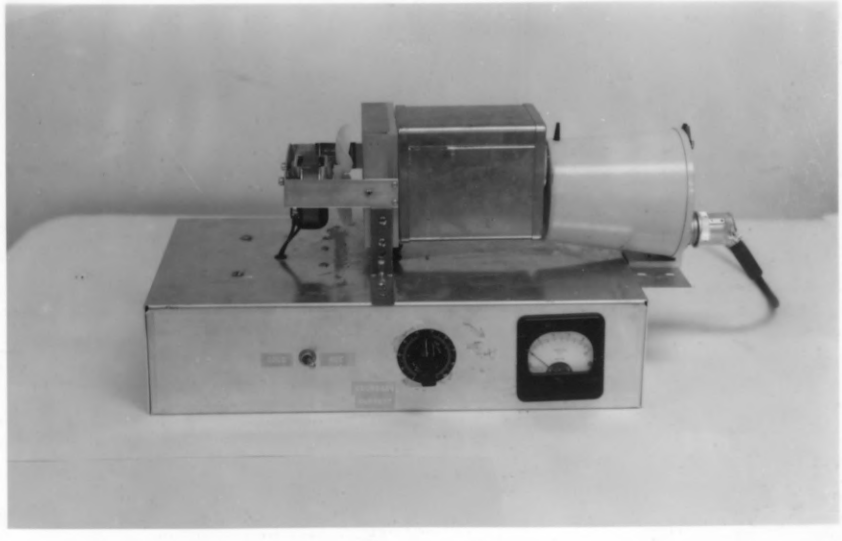

Figure 11. Detailed photo of electrically-controlled black body.

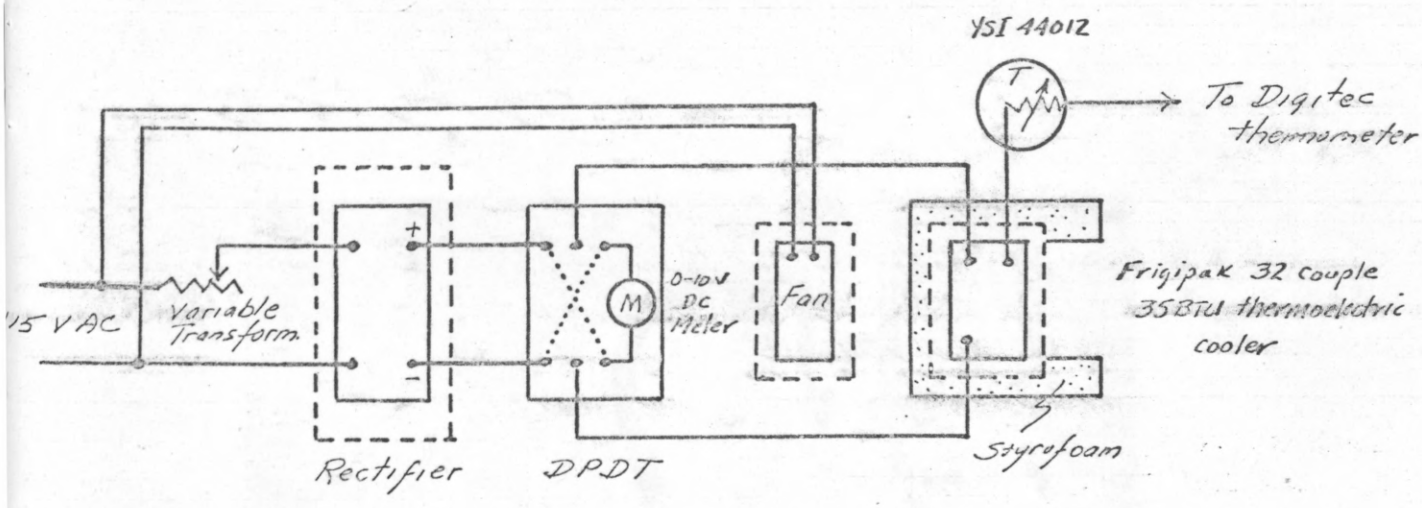

Figure 12. Wiring diagram of electrically controlled black body.

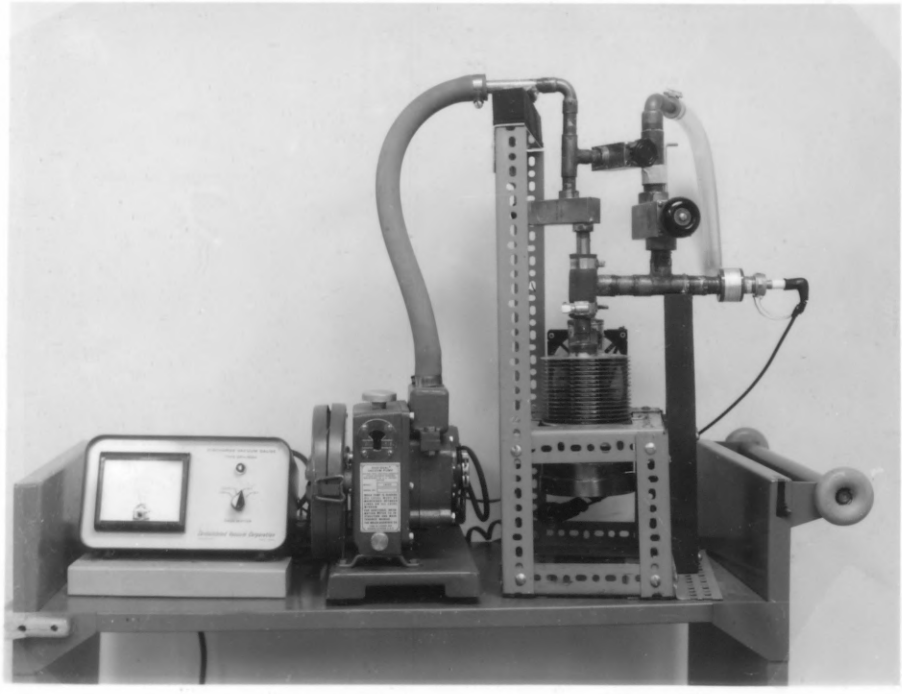

Figure 13. Photo of vacuum system for IR scanner showing vacuum gauge (left) roughing pump (center) and diffusion pump (right).

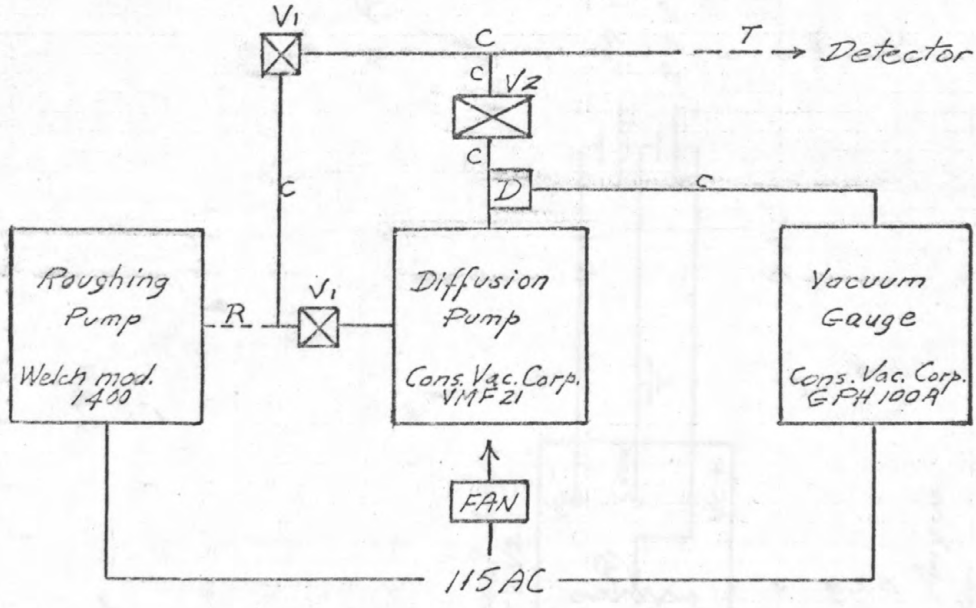

C = copper tubing
T = Tygon tubing
R = Rubber tubing
V_1 = VEECO FL62S
V2 = VEECO FL100S
D = Diode

Figure 14. Block diagram of vacuum system for IR scanner.

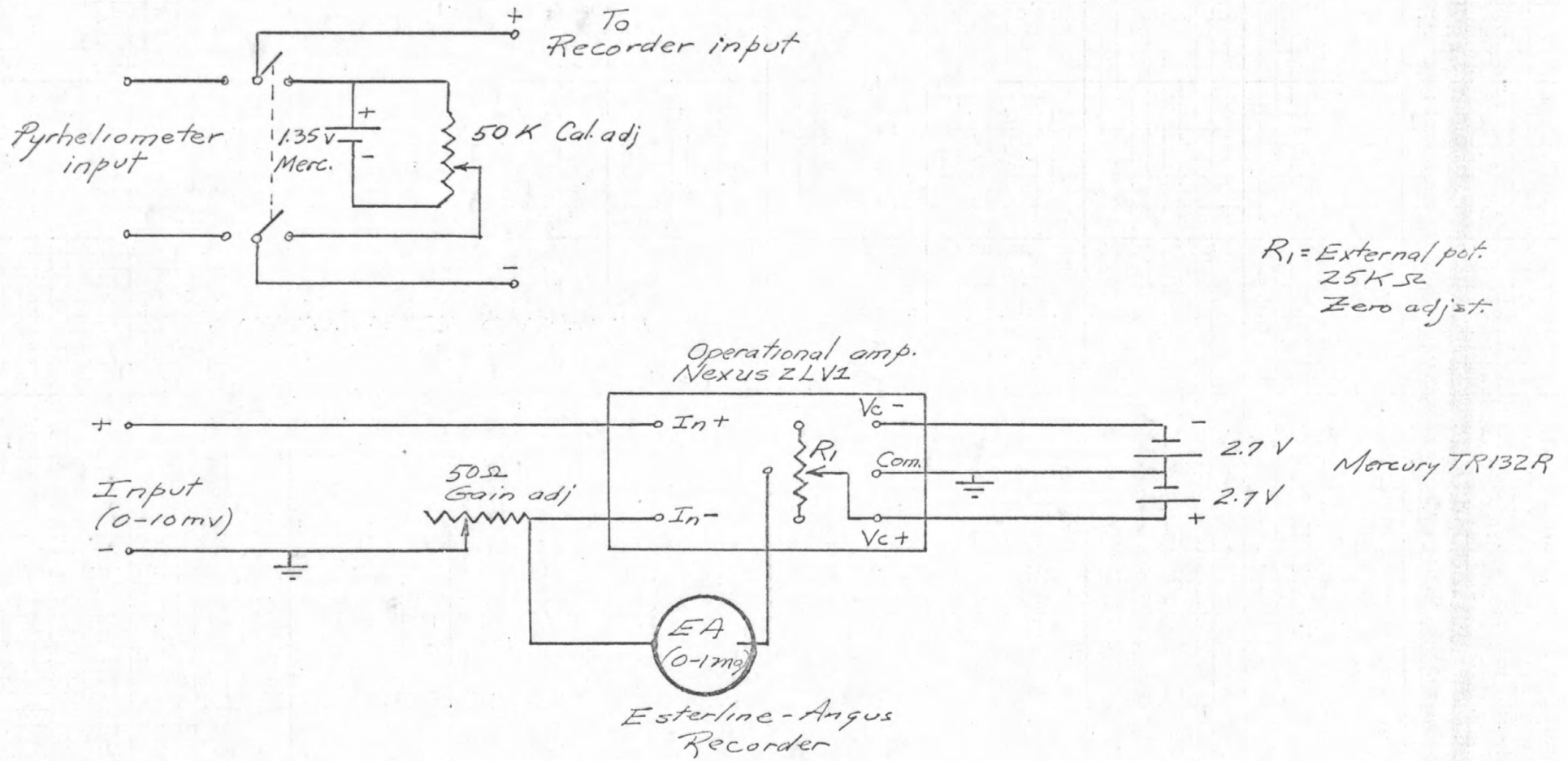

Figure 15. Amplifier for EA recorder (bottom) and pyrheliometer calibrator (upper left). These two circuits are combined (fig. 16) for field recording of pyrheliometer. The amplifier circuit is suitable for other uses, e.g. sequencing bridge.

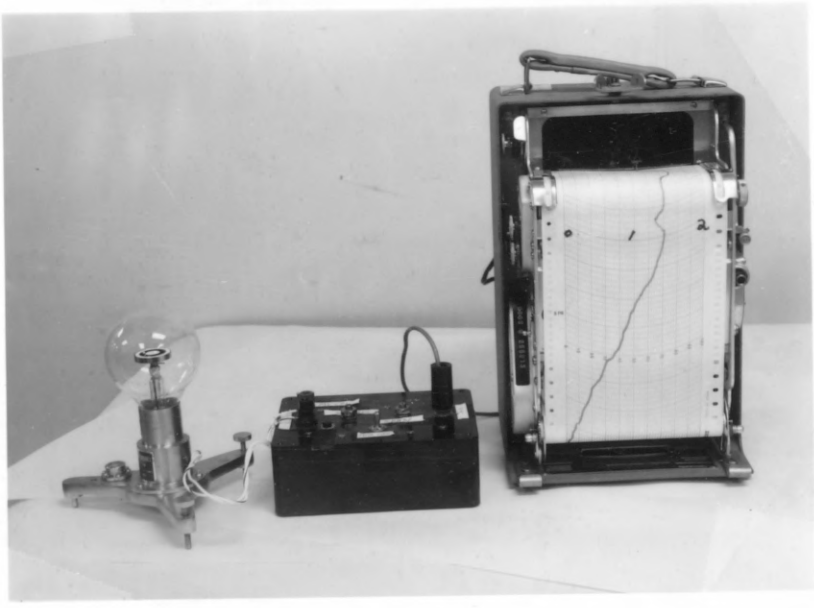

Figure 16. Photo of pyrheliometer (left) amplifier-calibrator (center) and EA recorder (right).

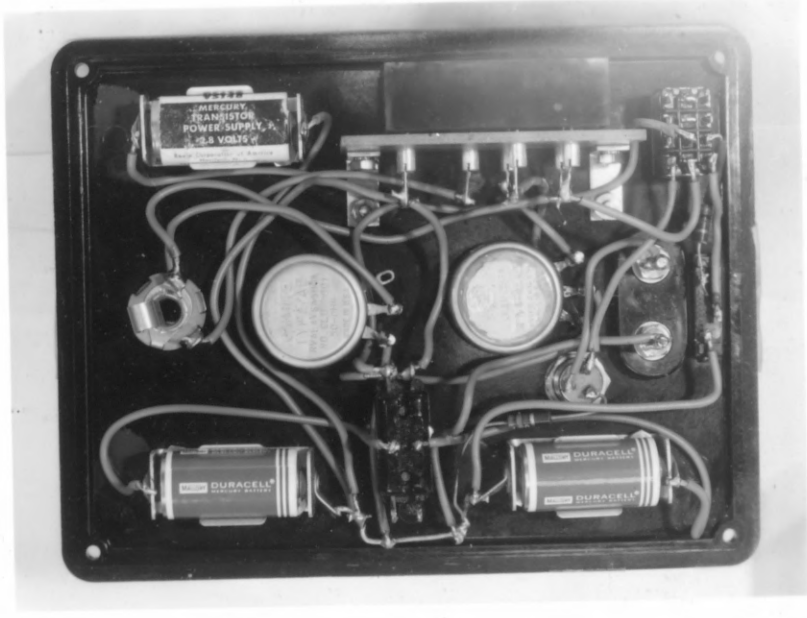

Figure 17. Photo of pyrheliometer calibrator-amplifier.

Figure 18. Graph showing time vs first light (CdS), sunrise (pyrheliometer) and surface temperature rise.

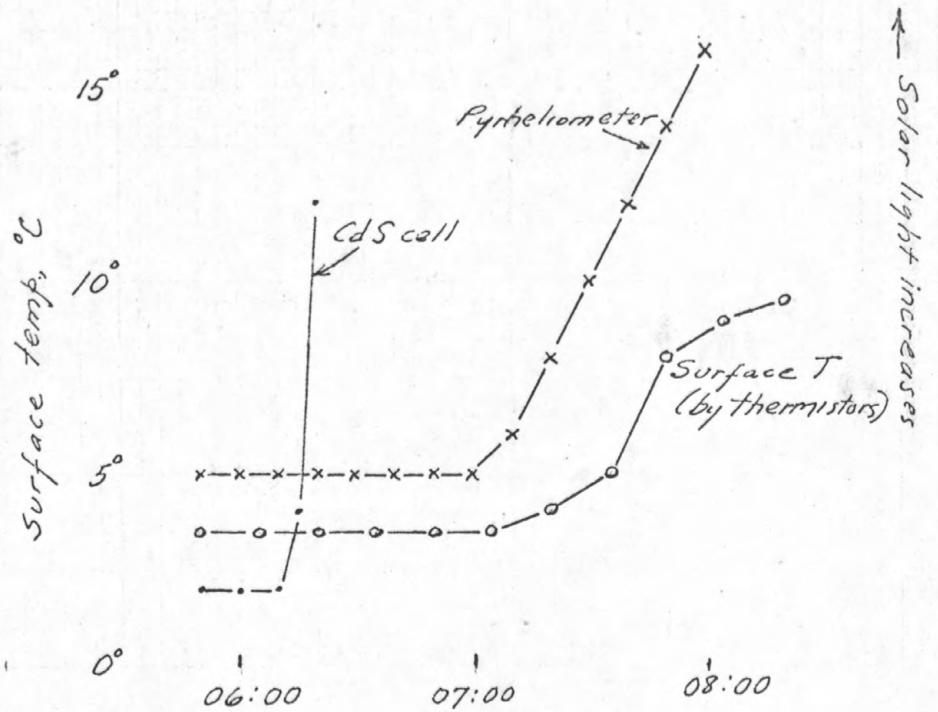

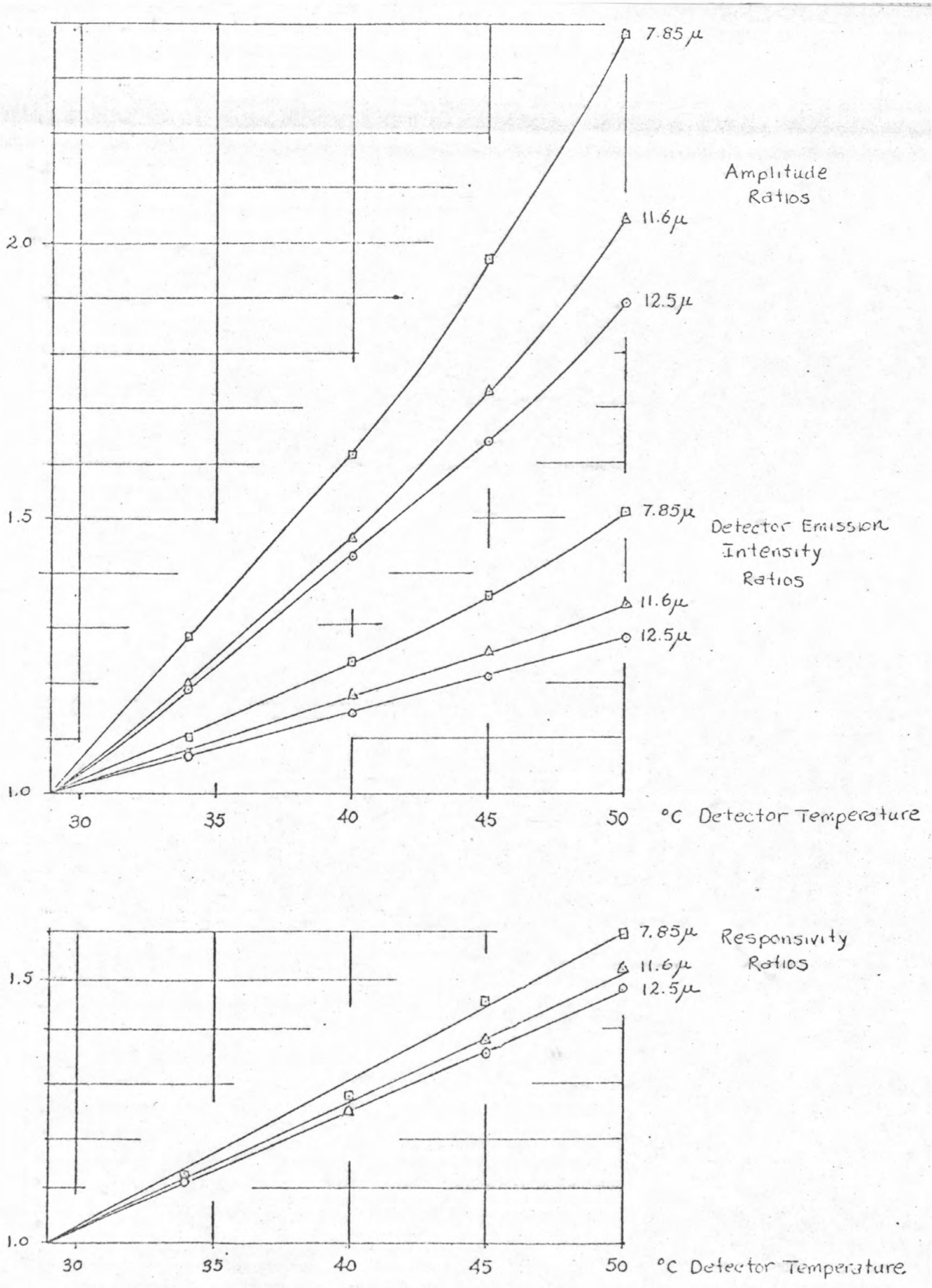

Figure 19. Graph showing performance of liquid nitrogen black body.

Fig. 41

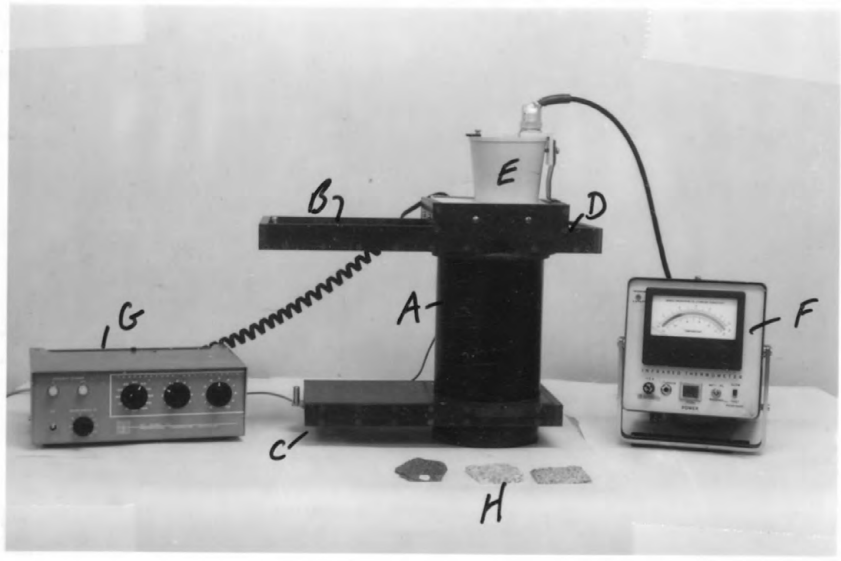

Figure 20. Emissivity measuring system. Emissivity box (A) with upper mirror (B), lower mirror (C) and heater (D). Radiometer head (E) is connected to radiometer (F) at right. The heater controller (G) is at the left. Three rock samples (H) prepared for laboratory testing are shown in foreground.

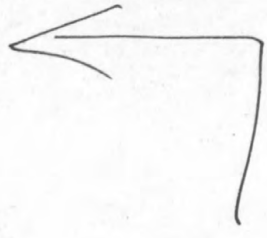

Figure 21. Thermal conductivity measuring system. Controlled temperature water baths (A) and (B) maintain a constant temperature gradient in stacks (C) and (D), shown with insulated jackets in place. Pressure is applied by hydraulic jack (E) and measured by means of gage (F). Thermistor circuits are selected by switch (G) and resistances measured by the Wheatstone bridge (H) and null detector (I).

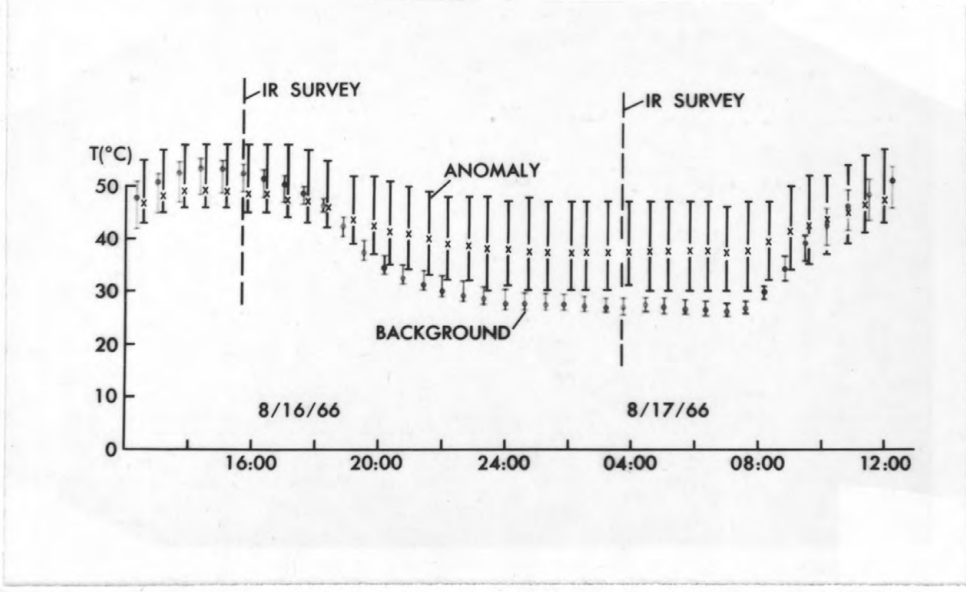

Figure 22. Graph showing anomaly and background surface temperatures measured with multiple probe sequencer at The Geysers.

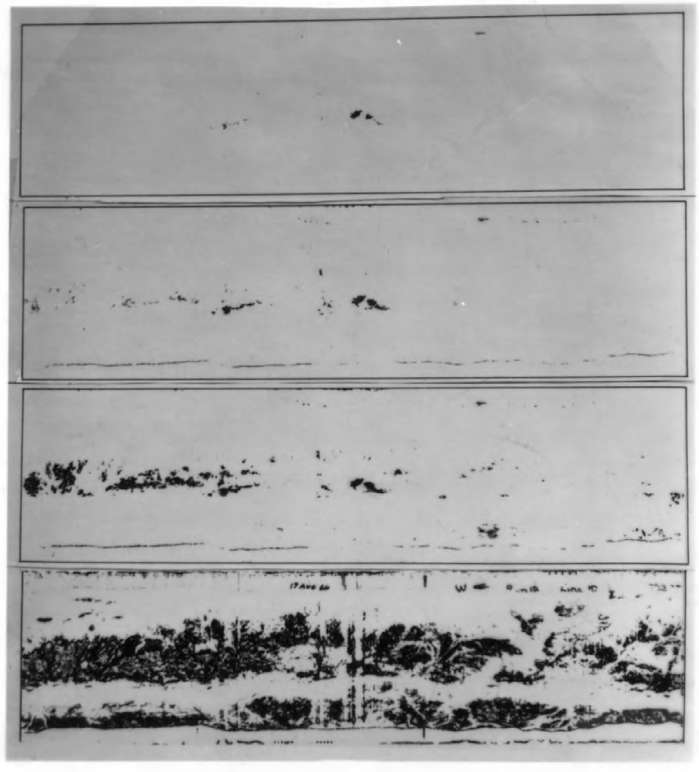

Figure 23. Four levels of density "sliced" with a Tech/Ops quantizer, from IR image of The Geysers. Hottest targets at top, cooler surfaces added by the succeeding three increments.

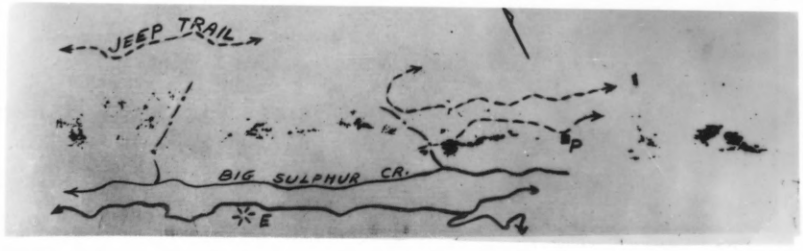

Figure 24. Geographic features superimposed upon level slice (fig. 23). Present northwestern steam production limit is about at center of image. Thermal anomalies extend beyond this limit.

Figure 26. IR image of Potomac River showing warm sewage plant effluent (A) and power plant effluent (B). (white=hot).

Figure 27. Infrared image of Balayan Bay, Luzon Island, Philippines.

Figure 25. IR images at Taal Volcano, Philippines (white=hot).

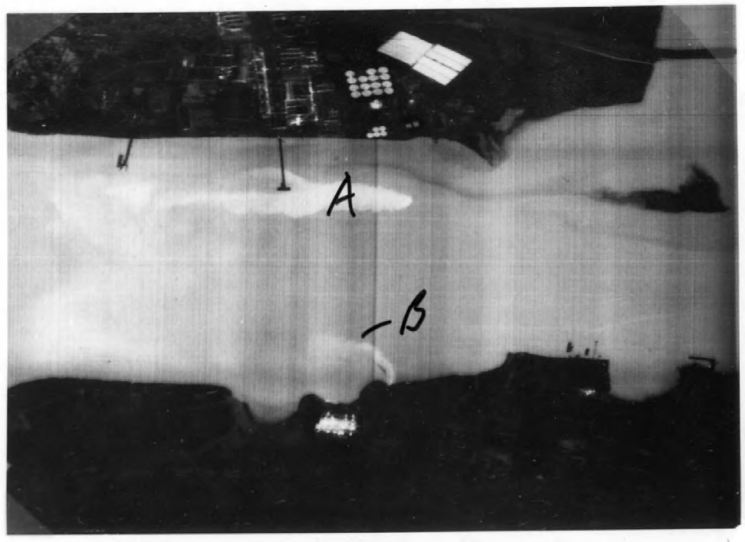

Figure 26. IR image of Potomac River showing warm sewage plant effluent (A) and power plant effluent (B). (white=hot).

Figure 27. Infrared image of Balayan Bay, Luzon Island, Philippines.

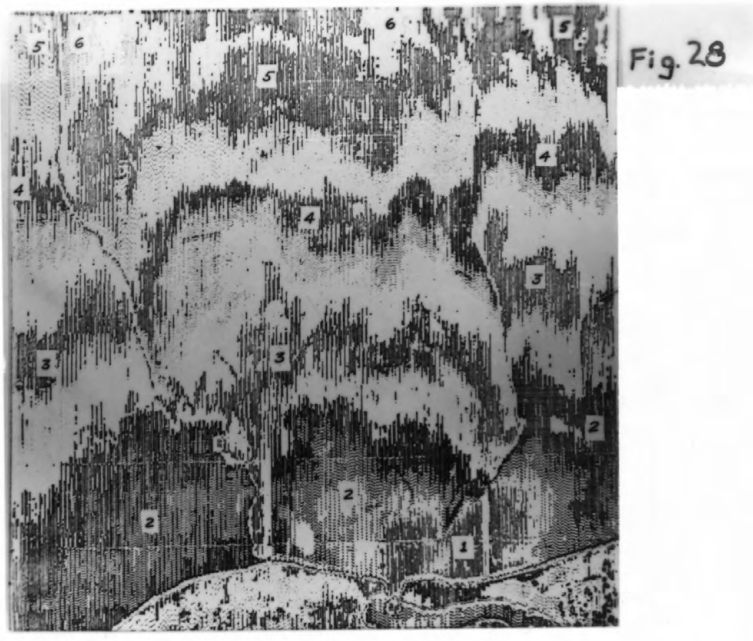

Figure 28. IDT black and white density map of fig. 27.

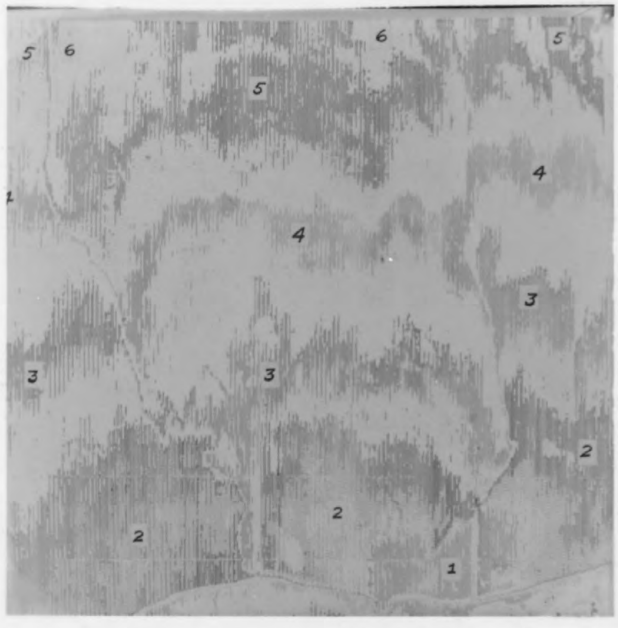

Figure 29. IDT color density map of fig. 27.

Figure 30. Rear view of MDT showing color attachment: A=light compartments. B=photocell housing. C=chassis. D="Dial-lite" spring clip attachment to recording pen arm.

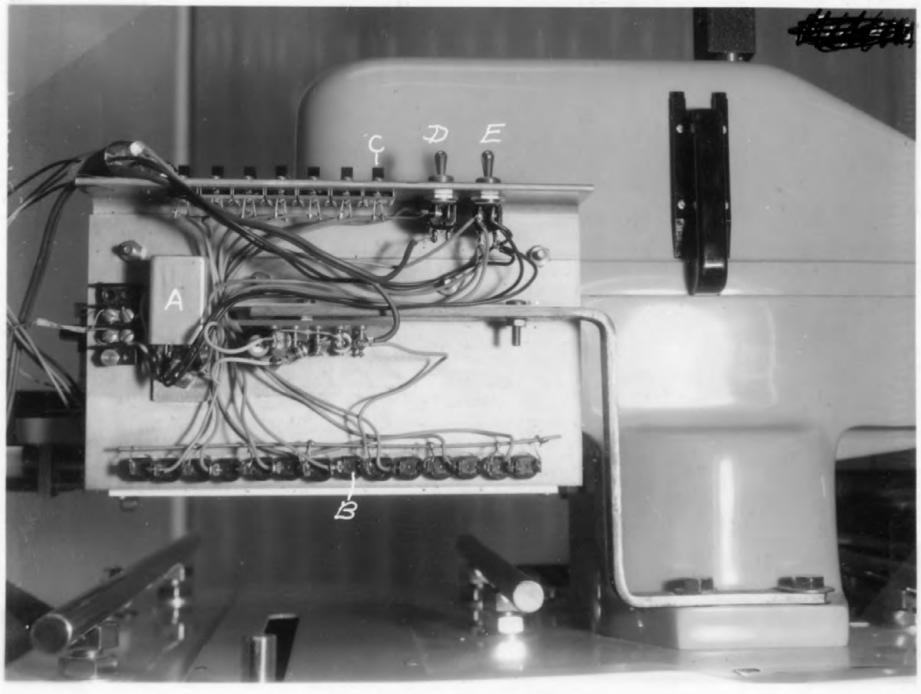

Figure 31. Side view of MDT showing color attachment: A=photocell relay. B=lamp socket. C=light compartment switch. D=main light switch. E=photocell circuit bypass switch. F=mounting bracket.

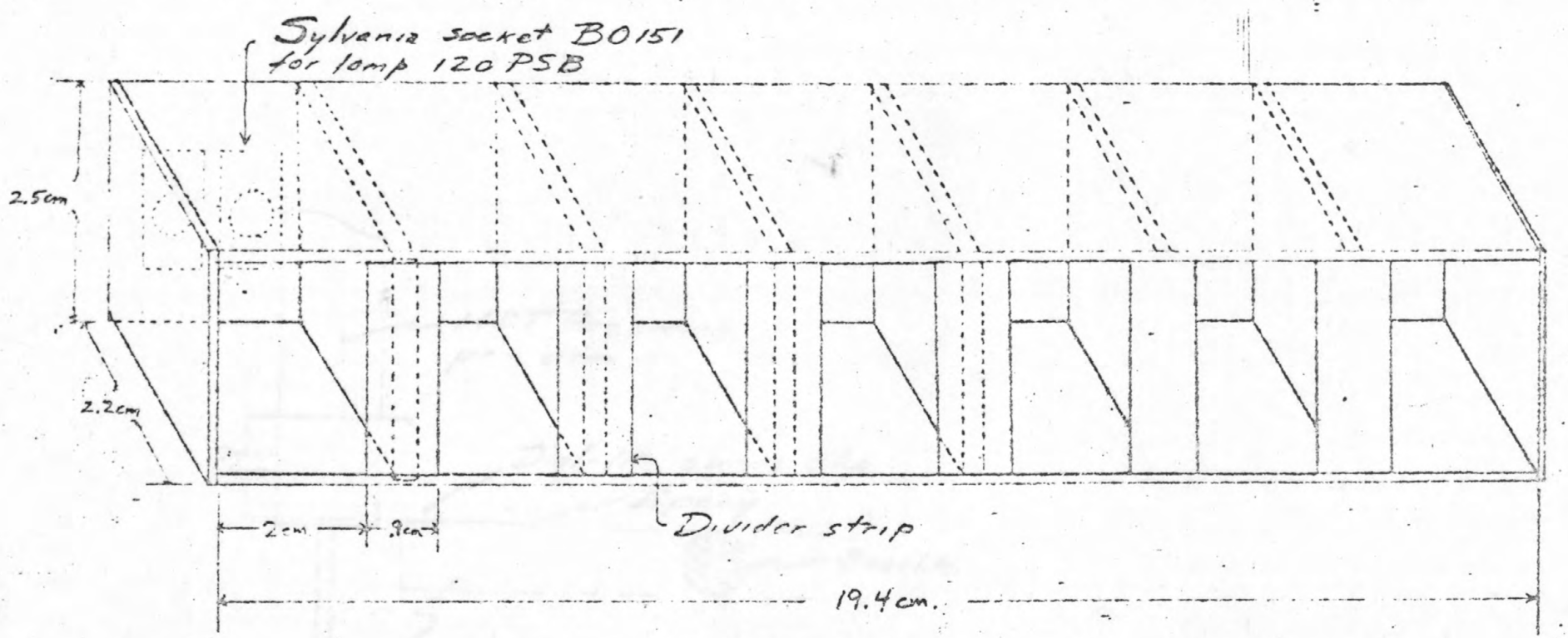
Sylvania socket BO151
for lamp 120 PSB
2.5cm
2.2cm
2cm
3cm
Divider strip
19.4cm.

Figure 32

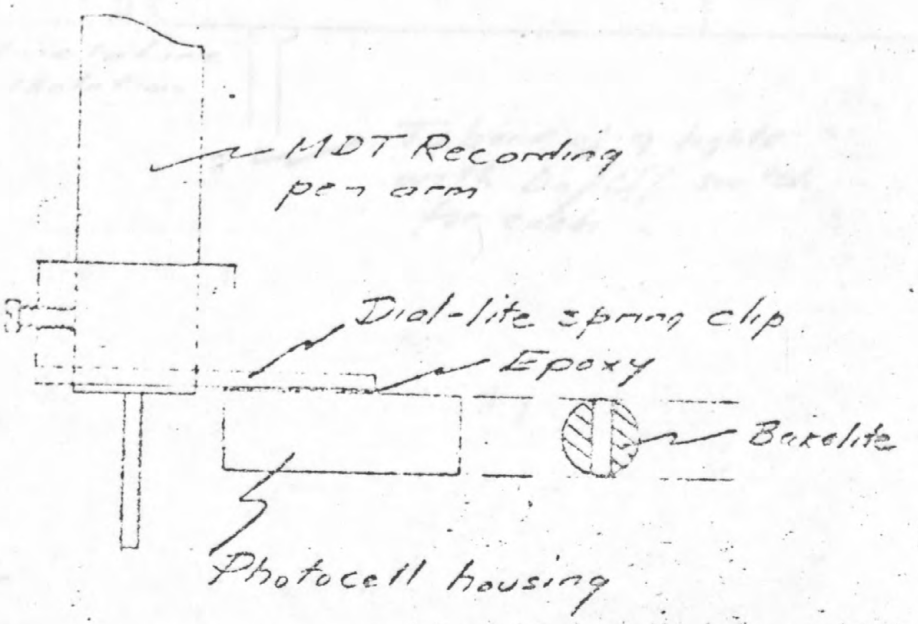
MDT Recording
pen arm
Dial-lite spring clip
Epoxy
Bakelite
Photocell housing

Figure 3B

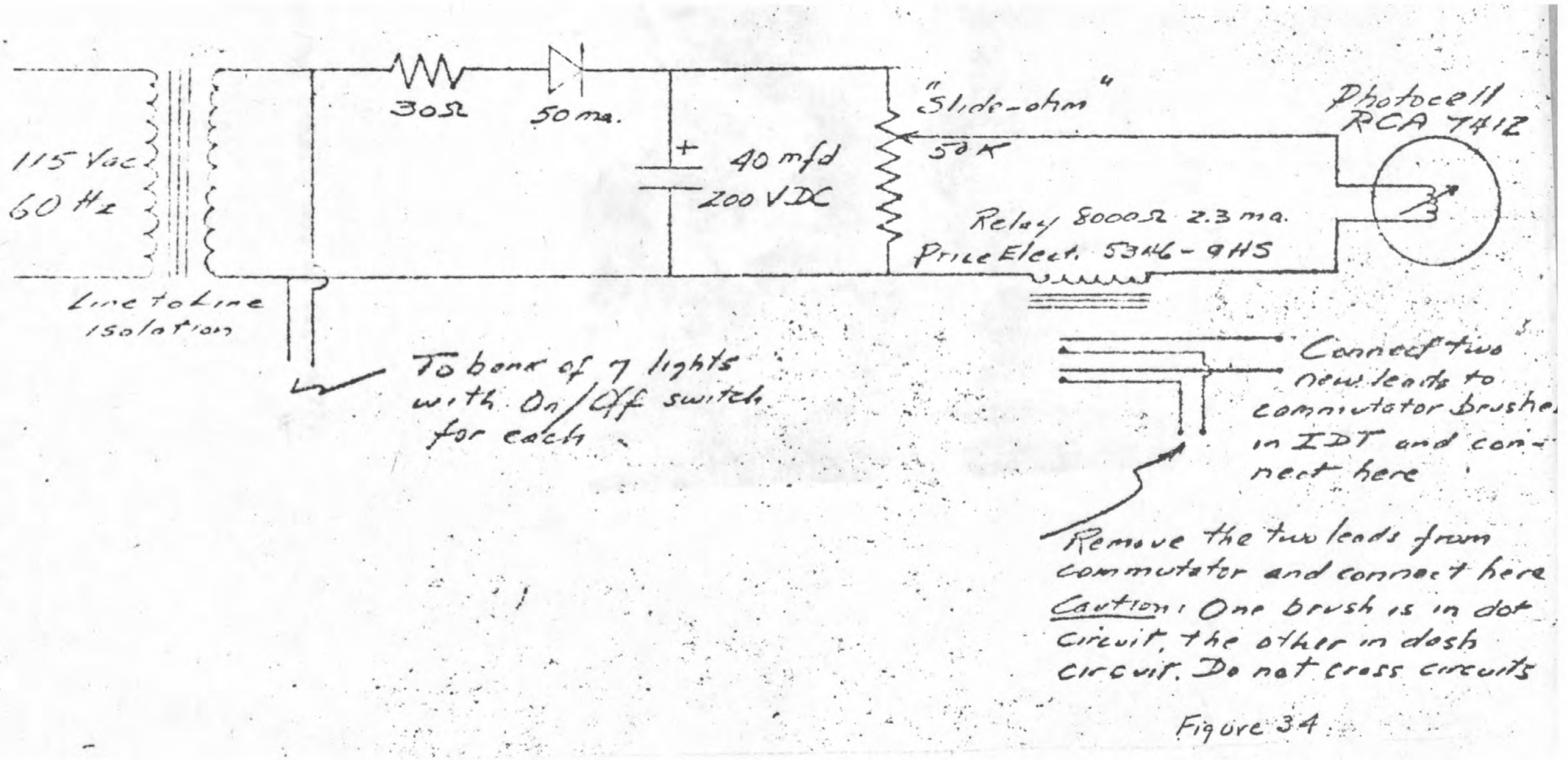
115 Vac
60 Hz
30Ω
50 ma.
+
40 mfd
200 V.DC
"Slide-ohm"
50K
Photocell
RCA 7412
Relay 8000Ω 2.3 ma.
Price Elect. 5346-9HS
Line to Line
Isolation
To bank of 7 lights
with On/Off switch
for each.
Connect two
new leads to
commutator brushes
in IDT and con-
nect here
Remove the two leads from
commutator and connect here
Caution: One brush is in dot
circuit, the other in dash
circuit. Do not cross circuits

Figure 34.

Figure 35. Tech/Ops density map of figure 27.